Fatty acid modulation and polyamine block of GluK2 kainate receptors analyzed by scanning mutagenesis

Timothy J. Wilding, Kevin Chen, and James E. Huettner

Department of Cell Biology and Physiology, Washington University Medical School, St. Louis, MO 63110

RNA editing of kainate receptor subunits at the Q/R site determines their susceptibility to inhibition by cis-unsaturated fatty acids as well as block by cytoplasmic polyamines. Channels comprised of unedited (Q) subunits are strongly blocked by polyamines, but insensitive to fatty acids, such as arachidonic acid (AA) and docosahexaenoic acid (DHA), whereas homomeric edited (R) channels resist polyamine block but are inhibited by AA and DHA. In the present study, we have analyzed fatty acid modulation of whole-cell currents mediated by homomeric recombinant GluK2 (formerly GluR6) channels with individual residues in the pore-loop, M1 and M3 transmembrane helices replaced by scanning mutagenesis. Our results define three abutting surfaces along the M1, M2, and M3 helices where gain-of-function substitutions render GluK2(Q) channels susceptible to fatty acid inhibition. In addition, we identify four locations in the M3 helix (F611, L614, S618, and T621) at the level of the central cavity where Arg substitution increases relative permeability to chloride and eliminates polyamine block. Remarkably, for two of these positions, L614R and S618R, exposure to fatty acids reduces the apparent chloride permeability and potentiates whole-cell currents ~5 and 2.5-fold, respectively. Together, our results suggest that AA and DHA alter the orientation of M3 in the open state, depending on contacts at the interface between M1, M2, and M3. Moreover, our results demonstrate the importance of side chains within the central cavity in determining ionic selectivity and block by cytoplasmic polyamines despite the inverted orientation of GluK2 as compared with potassium channels and other pore-loop family members.

The Journal of General Physiology

INTRODUCTION

Amphiphilic compounds, including the cis-unsaturated fatty acids arachidonic acid (AA) and docosahexaenoic acid (DHA), regulate the activity of ion channels, transporters, and a variety of other membrane proteins (Boland and Drzewiecki, 2008; Meves, 2008; Roberts-Crowley et al., 2009). In most cases the specific mechanism of regulation remains unknown, but it is thought to involve partition of the compounds into the membrane where they may alter the bulk mechanical properties of the bilayer (Bruno et al., 2007; Lundbaek, 2008; Phillips et al., 2009), displace annular lipids immediately surrounding the protein (Powl and Lee, 2007), or bind to specific domains along the protein–lipid interface (Grossfield et al., 2006; Gawrisch and Soubias, 2008). Despite these uncertainties, we have begun to use scanning mutagenesis to investigate how changes in the structure of glutamate receptors alter their susceptibility to modulation by free AA and DHA (Wilding et al., 2008). Members of the ionotropic glutamate receptor family are particularly attractive for this analysis because different family members may be potentiated, inhibited, or unaffected by exposure to AA or DHA, depending on their subunit composition and editing status. NMDA receptors, made up of GluN1 and GluN2 subunits (see Collingridge et al., 2009 for current IUPHAR subunit nomenclature), are potentiated after treatment with AA or DHA (Miller et al., 1992; Nishikawa et al., 1994), whereas neuronal α-amino-3-hydroxy-5-methyl-4-isoxazolepropionate (AMPA) receptors are weakly inhibited by AA (Kovalchuk et al., 1994). Currents mediated by native kainate receptors, as well as some recombinant receptors, are strongly inhibited by fatty acids (Wilding et al., 1998), although susceptibility of recombinant receptors to fatty acid inhibition depends on the editing status at the Q/R site within the channel pore (Wilding et al., 2005). Recombinant channels in which all of the subunits include an R at the Q/R site are inhibited by DHA, but inclusion of unedited subunits with Q at this location dramatically reduces inhibition (Wilding et al., 2005). Editing status at the Q/R site also governs the permeation properties of kainate and AMPA receptors and their susceptibility to pore block by polyamines. Channels homomeric for Q at the Q/R site exhibit more potent polyamine block (Bowie and Mayer, 1995; Kamboj et al., 1995; Koh et al., 1995) and higher relative permeability to calcium (Dingledine

Correspondence to James E. Huettner: jhuettner@wustl.edu

Abbreviations used in this paper: AA, arachidonic acid; AMPA, α-amino-3-hydroxy-5-methyl-4-isoxazolepropionate; DHA, docosahexaenoic acid.

The Rockefeller University Press $30.00
J. Gen. Physiol. Vol. 136 No. 3 339–352
www.jgp.org/cgi/doi/10.1085/jgp.201010442

et al., 1999) than channels that include one or more edited (R) subunits.

The recently solved crystal structure of homomeric AMPA receptor subunit GluA2 (Sobolevsky et al., 2009) revealed a tetrameric pore similar to an inverted potassium channel (Doyle et al., 1998), as was predicted (Wo and Oswald, 1995; Wood et al., 1995) based on sequence homology and analysis of subunit topology (Bennett and Dingledine, 1995; Hollmann et al., 1994). Although several portions of the AMPA receptor channel that face the cytoplasm, including the M1–M2 and M2–M3 loops, were not resolved in the GluA2 crystal structure (Sobolevsky et al., 2009), the overall layout of the GluA2 pore generally supports previous structural interpretations that relied on homology to the pore-loop motif of potassium channels and cyclic nucleotide-gated channels (Panchenko et al., 2001; Kuner et al., 2003). In particular, the Q/R editing site lies at the apex of the pore loop, preceded by an α-helical domain and is likely followed by the open coil that forms the selectivity filter (Sobolevsky et al., 2009).

Scanning mutagenesis studies have yielded several insights into the structural basis of GluK2 regulation by polyamines and DHA. Work by Mayer and colleagues (Panchenko et al., 2001) identified locations within the pore loop where amino acid substitution with alanine or tryptophan reduced, or in one case enhanced, channel block by polyamines. In addition, our previous work showed that R at the Q/R site was not unique in conferring sensitivity to inhibition by DHA (Wilding et al., 2008). Instead, substitution with R at several locations in the upstream pore helix of GluK2(Q) resulted in homomeric channels that were strongly inhibited by DHA. Collectively, these results suggest an important role for pore-loop conformation in determining channel sensitivity both to polyamines and to lipid-derived antagonists.

In the present study, we have analyzed DHA inhibition in homomeric GluK2(Q) channels containing 70 of the Ala and Trp substitution mutations generated by Mayer and colleagues (Panchenko et al., 2001). In addition, we have extended our Arg scan of the pore of GluK2(Q) (Wilding et al., 2008) to include substantial portions of the M1 and M3 transmembrane helical domains. Together with previous work, our results identify more than 30 gain-of-function substitutions: point mutations that confer susceptibility to strong DHA regulation on GluK2(Q) channels that otherwise exhibit little or no functional regulation by DHA. The distribution of these mutation sites defines three surfaces at the interface of the M1, M2, and M3 helices where Arg substitution at any single location converts GluK2(Q) from being insensitive to free DHA to being strongly inhibited. Although our results do not directly address whether modulation involves specific binding of DHA to the channel, they demonstrate that positive charge anywhere along the contact surface between the pore helix and adjacent M1 and M3 helices leads to reduced channel activity in the presence of DHA, suggesting that DHA impedes the relative movement of M1, M2, and M3 associated with opening of wild-type channels that have undergone Q to R editing or mutant channels bearing specific Arg, Trp, or Ala substitutions along this interface domain. In addition, we have identified several positions along one face of the M3 helix at the level of the central cavity where substitution with Arg yields channels that are permeable to chloride as well as monovalent cations; for two of these Arg substitution mutants, exposure to DHA reduced relative chloride permeability and potentiated, rather than inhibited, whole-cell current amplitude. Collectively, our results suggest that exposure to DHA alters the relative orientation of M3 in the open state, changing which face of the helix is directed toward the central cavity. Finally, the persistence of DHA modulation in the near absence of internal polyamines, as well as the incomplete overlap in sites where amino acid substitution alters polyamine block and DHA modulation, indicates that polyamines are not required for channel regulation by DHA.

MATERIALS AND METHODS

cDNA constructs, cell culture, and transfection

Wild-type GluK2(R) cDNA (Egebjerg et al., 1991), provided by Steve Heinemann (Salk Institute, La Jolla, CA), was subcloned into the pcDNA3 vector for expression in HEK293 cells. Mark Mayer provided alanine and tryptophan substitution mutants of GluK2(Q): D567A through S601A and D567W through R603W (Panchenko et al., 2001). Additional point mutations were prepared by site-directed mutagenesis using the QuickChange II XL kit (Agilent Technologies), as previously described (Wilding et al., 2008), and verified by sequencing. HEK 293 cells at ∼60% confluence were transfected with 1–3 μg of subunit cDNA using Superfect reagent (QIAGEN) or lipofectamine (Invitrogen) according to the manufacturer's protocols. For most experiments, cells were cotransfected with a second plasmid encoding green fluorescent protein (pEGFP, Takara Bio Inc.). On the day after transfection, cells were dissociated with mild protease treatment and replated at low density on nitrocellulose-treated 35-mm dishes (Wilding et al., 2008). Physiological recordings were obtained from GFP-expressing cells 24–48 h after replating.

Electrophysiology

Cultures were perfused continuously with Tyrode's solution (in mM): 150 NaCl, 4 KCl, 2 $MgCl_2$, 2 $CaCl_2$, 10 glucose, 10 HEPES, pH 7.4 with NaOH. Whole-cell electrodes had an open tip resistance of 1–5 MOhm when filled with internal solution (in mM): 140 cesium glucuronate, 10 EGTA, 5 CsCl, 5 $MgCl_2$, 5 ATP, 1 GTP, 0.02 spermine, and 10 HEPES, pH adjusted to 7.4 with CsOH. For some experiments, spermine was left out of the internal solution and ATP concentration was increased to 20 mM to buffer endogenous polyamines (Rozov et al., 1998). Currents were recorded with an Axopatch 200A amplifier, filtered at 1–2 kHz, and digitized at 5–10 kHz with a Digidata 1300 interface and p-Clamp software. For most experiments, the cells were pretreated with 2 μM concanavalin A for 5 to 10 min to increase steady-state agonist responses (Huettner, 1990). Once the whole-cell mode was attained, a multi-barreled local perfusion pipette was used to

deliver agonists dissolved in control extracellular solution (in mM): 160 NaCl, 2 $CaCl_2$, 10 HEPES, pH 7.4 with NaOH. For experiments that required rapid solution exchange, the drug reservoirs were kept under ~10 p.s.i. of static air pressure, and computer-gated electronic valves were used to control solution flow to the delivery pipette. Because of the relatively small maximal amplitude of currents mediated by mutant subunits, whole-cell recordings were used to analyze desensitization, despite unavoidable limitations on the speed of extracellular solution exchange (tau ~5–15 ms).

DHA stocks (50 mM in DMSO) were stored at −80°C in aliquots under argon gas and freshly diluted each day for recording. Inhibition or potentiation by DHA was quantified as the ratio of kainate-evoked current immediately after 2–3-min exposure to 15–30 µM DHA in external solution, to the control current before DHA treatment. Whether inhibited or potentiated by DHA, currents typically recovered to control amplitudes after 3–5-min wash with 0.1% BSA in control external solution (Wilding et al., 1998).

Data analysis

Current–voltage relations were generated by ramping the membrane potential with a triangle wave from −150 or −120 mV to +120 mV at ~1 mV/ms. Averages of five ramps, recorded in control solution immediately before or after exposure to kainate, were subtracted from the mean ramp current during kainate application. In most recordings there was little or no hysteresis between rising and descending ramps, thus interaction with polyamines was assumed to be at steady state (see Rozov et al., 1998). Chord conductance (G) was calculated from $G = I/(V_m - V_{rev})$, where I is whole-cell current, V_m the membrane potential, and V_{rev} the reversal potential. Plots of G versus V_m were fit with an equation that incorporates two Boltzmann relations to describe inhibition by a permeant blocker (Panchenko et al., 2001 and references therein): $G = G_{max}/(1 + (1/B))$, where $B = \exp(-(V_m - V_b)/k_b) + \exp((V_m - V_p)/k_p)$, G_{max} is the maximal conductance, and V_b, V_p, k_b, and k_p are the midpoint voltages and slope factors for polyamine block and permeation, respectively. The voltage-independent polyamine dissociation constant ($K_{d(0)}$) was estimated from (Panchenko et al., 2001): $K_{d(0)} = [\text{spermine}] * (\exp(V_b/k_b) + \exp(-V_p/k_p))$. Mutants with IV relations that displayed little or no biphasic rectification, or with only outward rectifying IV relations, were designated as having Kd(0) > 100 µM (see Panchenko et al., 2001).

Permeability for chloride (P_{Cl}) relative to Cs (P_{Cs}) was calculated from the change in reversal potential when extracellular NaCl was replaced with sodium glucuronate (160 mM sodium glucuronate, 10 mM HEPES, 2 mM $CaCl_2$, pH adjusted to 7.4 with NaOH) using the following rearrangement of the Goldman-Hodgkin-Katz zero current equation (Hille, 2001): $P_{Cl}/P_{Cs} = ([Cs]_{in} * (X_1 - X_2))/(X_2 * [Cl]_{out\,2} - X_1 * [Cl]_{out\,1})$, where $X = 10\text{^}(V_{rev}/58.2\text{ mV})$ in NaCl (X_1) or sodium glucuronate (X_2); $[Cs]_{in}$ is the internal Cs concentration (150 mM); $[Cl]_{out}$ 1 and 2 are the external chloride concentrations in NaCl and sodium glucuronate, 164 mM and 4 mM, respectively (E_{Cl} = −60.5 and +33.4 mV). Additional evidence for Cl permeability came from recordings using a CsCl internal solution (in mM): 100 CsCl, 10 EGTA, 40 HEPES, 2.5 $MgCl_2$, 1.5 $CaCl_2$, pH to 7.0 with tetraethylammonium hydroxide (Wilding et al., 1995), for which E_{Cl} = −10.6 mV with extracellular NaCl.

Fluctuations in currents evoked by bath application of 10 µM kainate were analyzed as previously described (Wilding et al., 2008). Plots of steady-state current variance (σ^2), calculated over 1-s time intervals, versus mean current (I) were fit with the following parabolic equation (Sigworth, 1980): $\sigma^2 = i * I - I^2/N$, where i is the estimated unitary current amplitude and N is the estimated number of channels. Open probability was estimated as the ratio $P_o = I_{max}/(i * N)$, where I_{max} is the maximal mean whole-cell current. The number of channels (N) was assumed to be unchanged by acute exposure to DHA. All results are presented as mean +/− sem unless otherwise stated. Statistical significance was assigned at $P < 0.05$.

Molecular modeling

Homology modeling of a homomeric GluK2(Q) tetramer to the GluA2 crystal structure (PDB ID: 3KG2) was performed using Modeller (Sali and Blundell, 1993; Eswar et al., 2008) release 9v7, available at http://salilab.org/modeller/modeller.html. Sequence alignment of GluK2 and GluA2 in Fig. S2 of Sobolevsky et al. (2009) was used with additional twofold symmetry restraints imposed for the A, C and B, D chain pairs. The M1–M2 and M2–M3 loops were further refined by the high resolution discrete optimized protein energy (DOPE-HR) method (Shen and Sali, 2006).

Online supplemental material

The online supplemental material (available at http://www.jgp.org/cgi/content/full/jgp.201010442/DC1) contains three figures illustrating current–voltage relations for several M3 Arg substitution mutants (Fig. S1), analysis of polyamine block for M2 Arg substitution mutants (Fig. S2), and recordings performed under nominally polyamine-free conditions (Fig. S3).

RESULTS

Our previous analysis of Arg substitutions in the GluK2(Q) subunit spanning the range from V571 through P597 (Wilding et al., 2008) revealed a striking pattern of locations where replacement with Arg rendered homomeric GluK2(Q) channels susceptible to inhibition by DHA (Fig. 1). Based on homology to GluA2 and to the membrane-embedded domains of potassium channel subunits, our earlier study showed that Arg substitutions in M2 where the side chain was oriented toward the M1 and M3 transmembrane α helices significantly enhanced DHA inhibition. These results suggested that susceptibility to DHA may depend on interactions between the M2 helix and adjacent helices but did not rule out other possible mechanisms. For example, altered sensitivity to DHA might result from a local conformational change within M2 that did not involve any substantial change in contact with M1 and/or M3. To gain a better understanding of the structural basis for channel regulation by DHA we analyzed inhibition of homomeric channels formed by 70 Ala and Trp substitution mutants provided by Mark Mayer (Panchenko et al., 2001). Substitution with Ala provides a small nonpolar side chain that represents a conservative replacement for most small residues, and is likely to be tolerated at positions occupied by hydrophobic residues. In contrast, the large Trp side chain would be expected to induce local structural changes when replacing a variety of smaller residues. We also generated 58 new Arg substitution mutants that extend our scan of the GluK2 pore along major segments of the M1 and M3 helices. The large positively charged Arg side chain was chosen because Arg replaces Gln in wild-type edited subunits. Thus, Arg substitution mutants effectively move the Arg

side chain from position 590 to a different location within the channel domain of GluK2(Q). Most experiments were performed on cells that were pretreated with concanavalin A, to increase the amplitude of steady-state whole-cell currents (Huettner 1990).

Alanine scan of the GluK2(Q) pore loop

Similar to wild-type GluK2(Q), 15 μM DHA failed to inhibit homomeric channels formed by most subunits with alanine substituted at locations between D567 and R603. Only at two locations did replacement with alanine result in greater than ∼80% inhibition by DHA: T576 and F583 (Fig. 2 C). More modest inhibition (∼60–80%) was observed with Ala substitutions at F575, Q591, or P597 (see also Wilding et al., 2008). Among these residues, only F583A produced nearly complete relief from polyamine block of GluK2(Q) (Fig. 2 D) (Panchenko et al., 2001). Ala substitution at the other locations decreased the potency of intracellular spermine block by ∼3–12-fold (Panchenko et al., 2001). In addition, Ala substitution at two downstream positions that eliminate polyamine block, G592 and E594, had almost no effect on inhibition by DHA (Fig. 2 D). Together, these results indicate only weak correlation between locations where Ala substitution increases DHA inhibition or reduces polyamine block (Fig. 2, D and E; see Discussion).

Tryptophan scan of the GluK2(Q) pore loop

In contrast to alanine substitution, which only conferred susceptibility to DHA inhibition at a few locations, amino acid replacement with the larger tryptophan side chain yielded strong DHA inhibition at many positions in the pore helix preceding the Q/R site and at two positions, S593 and P597, in the downstream presumed open coil that forms the selectivity filter (Fig. 3). Upstream of the Q/R site substitution with Trp resulted in strong DHA inhibition and essentially complete relief of polyamine block (Panchenko et al., 2001) at the same five locations: T576, N579, S580, G584, and G586 (Fig. 3, C and D). Replacement with Trp at three additional sites A587, L588, and M589 immediately upstream of position 590 also strongly enhanced DHA inhibition and produced a 10–20-fold reduction in polyamine

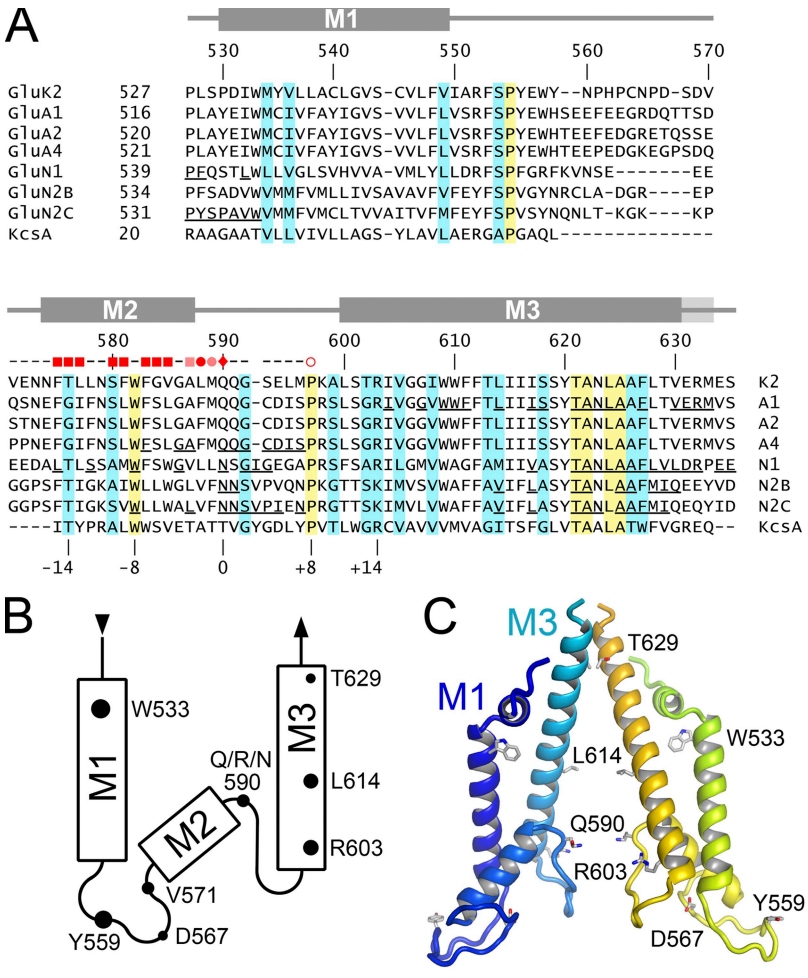

Figure 1. Homology among glutamate receptor and potassium channel subunits. (A) Amino acid sequence alignments of GluK2 with AMPA receptor subunit GluA1, GluA2, and GluA4, NMDA receptor subunits GluN1, GluN2B, and GluN2C, and potassium channel subunit KcsA. Yellow and light teal shading indicate positions with amino acid identity or conservative substitutions, respectively, with the following groups as conservative replacements: (A, C, G, S, T), (I, L, M, V), (F, W, Y), (H, K, R). Gray shaded boxes above the alignment indicate the presumed extent of the pore-loop helix (M2) and downstream transmembrane α helix (M3) based on homology to the GluA2 crystal structure. Residues are numbered for the mature GluK2 protein. Underlined residues in GluA1 (Sobolevsky et al., 2003), GluA4 (Kuner et al., 2001), GluN1 (Kuner et al., 1996; Beck et al., 1999), GluN2B (Chang and Kuo, 2008), and GluN2C (Kuner et al., 1996; Sobolevsky et al., 2002), when substituted with Cys, exhibit modification by methanethiosulfonate reagents applied from either the cytoplasmic (M2 residues) or extracellular (M3 residues) solutions. Symbols immediately above the alignment denote locations where Arg substitution strongly (dark red) or weakly (light red) enhanced susceptibility of GluK2(Q) to DHA inhibition (see Wilding et al., 2008). Squares, presumed α-helical residues; circles, presumed open coil residues; diamond, the Q/R/N site; filled symbols, upstream locations; open symbols, downstream. (B) Membrane topology of glutamate receptor subunit M1–M3 domain. Subunits were analyzed with single Ala and Trp point mutations between residues D567 and R603, and with Arg substitutions between residues W533-Y559 and V571-T629. (C) Homology model of the GluK2 M1–M3 domain; two non-adjacent subunits are shown.

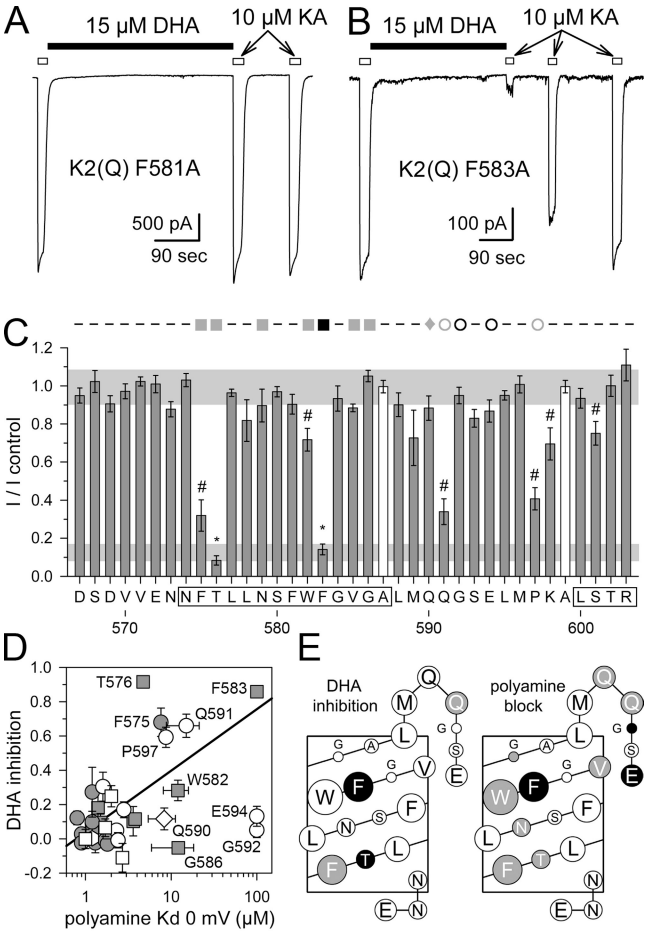

Figure 2. Pore-loop locations where Ala substitution enhances DHA inhibition of GluK2(Q). Whole-cell currents evoked by 10 μM kainate before and after exposure to 15 μM DHA in Con A–treated HEK cells expressing homomeric GluK2(Q) receptors with Ala substitutions at F581 (A) or F583 (B). (C) Current evoked by the first kainate application after exposure to DHA plotted as a fraction of control current before DHA. *, significantly different from Q590 but not Q590R, one-way ANOVA on ranks, $P < 0.05$ by Dunn's method of post-hoc comparison to control. #, significantly different from both Q590 and Q590R, rank sum test, $P < 0.05$. Symbols above the plot denote locations where Ala substitution produced a strong (black) or intermediate (gray) reduction in polyamine block of GluK2(Q) (see Panchenko et al., 2001). Squares, presumed α-helical residues; circles, presumed open coil residues; diamond, the Q/R/N site; filled symbols, upstream locations; open symbols, downstream. (D) DHA inhibition (1 – I/Icontrol) plotted versus polyamine Kd calculated at 0 mV. Upstream residues are shaded, downstream are open. Correlation coefficient from linear regression of the upstream residues was 0.66. (E) Net diagrams of the pore helix and adjacent residues. Circle diameter for each residue proportional to side chain volume. (Left) Filled circles indicate locations where Ala substitution allowed strong (black) or intermediate (gray) inhibition by DHA (Right) Filled circles indicate strong (black) or intermediate (gray) reduction in polyamine block when substituted by Ala.

block (Panchenko et al., 2001). Thus, for Trp replacement of upstream residues there is almost perfect agreement between reduction in polyamine block and enhancement of inhibition by DHA. Notably, Trp substitution at wild-type residues with small side chain volumes (Gly, Ala, Ser, Thr, and Asn) strongly affected both DHA inhibition and polyamine block in parallel (Fig. 3 E). However, Trp substitution at the Q/R site and immediate downstream residues did not show good correlation between DHA inhibition and polyamine block. GluK2 Q590W exhibited intermediate inhibition by DHA (Fig. 3) and enhanced block by polyamines (Panchenko et al., 2001). Trp substitution for Q591, S593, and P597 resulted in intermediate to strong inhibition by DHA but weak relief of polyamine block. In contrast, Trp substitutions at G592 and E594, which eliminate polyamine block, did not strongly enhance DHA susceptibility. Collectively, these results suggest that effective polyamine block strongly depends on the conformation of both the selectivity filter domain and the upstream pore helix, whereas residues immediately downstream of the Q/R site play a more limited role in DHA inhibition of the channel (see also Wilding et al., 2008).

Arginine substitutions in M3

Our previous analysis with Arg substitutions in the M2 helix indicated that Arg residues directed toward the M1and M3 helices increased susceptibility to inhibition by DHA. This observation led us to test whether Arg substitutions in M1 or M3 might also increase susceptibility to DHA via displacement of M2. As shown in Fig. 4, Arg was less well tolerated in M3 than in the pore loop, as indicated by the higher proportion of substitution mutants that failed to express as functional channels (X). Nevertheless, many of the mutant subunits that did produce functional homomeric channels exhibited altered susceptibility to DHA compared with wild-type GluK2(Q). Four of the functional M3 Arg substitution mutants (T602R, G606R, G607R, and W610R), clustered within ~2.2 helical turns, were strongly inhibited by exposure to DHA (Fig. 4 C). Surprisingly, however, substitutions at three locations (L600R, L614R, and S618R) yielded receptors that were potentiated. The effect of DHA on L600R was modest (1.4 ± 0.1 of control, $n = 14$ cells, $P < 0.001$), but for the L614R and S618R substitutions, exposure to DHA increased the steady-state current by 4.8 ± 0.4-fold ($n = 41$, $P < 0.001$) and 2.3 ± 0.3-fold ($n = 25$, $P < 0.001$), respectively.

Several of the positions where Arg substitution resulted in apparently nonfunctional channels were located near R603 at the cytoplasmic end of M3 (Fig. 1 B and Fig. 4 C). Because dibasic RR and RXR motifs can serve as a signal for protein retention in the ER (Margeta-Mitrovic et al., 2000), we were concerned that lack of expression for these mutants might be an indirect effect of ER retention, rather than a direct result of local interactions by the arginine side chain. ER retention does not explain the poor expression of these subunits, however, because replacing R603 with W, which

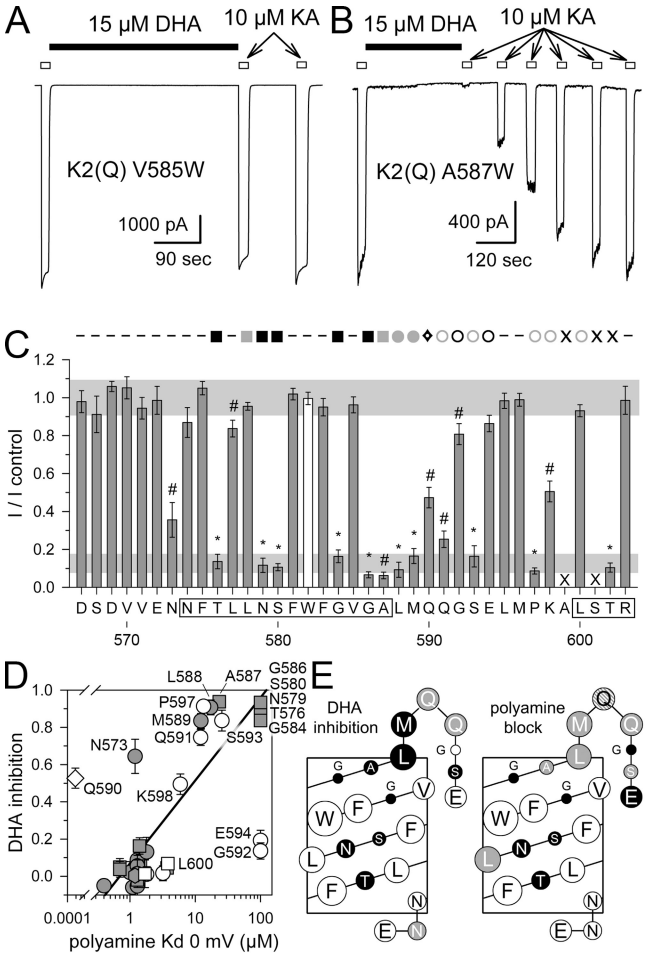

Figure 3. Pore-loop locations where Trp substitution enhances DHA inhibition of GluK2(Q). Whole-cell currents evoked by 10 μM kainate before and after exposure to 15 μM DHA in Con A–treated HEK cells expressing homomeric GluK2(Q) receptors with Trp substitutions at V585 (A) or A587 (B). (C) Current evoked by the first kainate application after exposure to DHA plotted as a fraction of control current before DHA. *, significantly different from Q590 but not Q590R, one-way ANOVA on ranks, $P < 0.05$ by Dunn's method of post-hoc comparison to control. #, significantly different from both Q590 and Q590R, rank sum test, $P < 0.05$. Currents for Trp substitution at A599 or S601 were too small to analyze (X). Symbols above the plot denote locations where Trp substitution produced a strong (black) or intermediate (gray) reduction in polyamine block of GluK2(Q) (see Panchenko et al., 2001). Squares, presumed α-helical residues; circles, presumed open coil residues; diamond, the Q/R/N site; filled symbols, upstream locations; open symbols, downstream. (D) DHA inhibition (1 – I/Icontrol) plotted versus polyamine Kd calculated at 0 mV. Upstream residues are shaded, downstream are open. Correlation coefficient from linear regression of the upstream residues was 0.90. (E) Net diagrams of the pore helix and adjacent residues. Circle diameter for each residue proportional to side chain volume. (Left) Filled circles indicate locations where Trp substitution allowed strong (black) or intermediate (gray) inhibition by DHA. (Right) Filled circles indicate strong (black) or intermediate (gray) reduction in polyamine block when substituted by Trp.

by itself had no effect on DHA inhibition (Fig. 3), did not rescue expression of S601R, I604R, or V605R (Fig. 4 E). In addition, the T602R substitution enhanced DHA inhibition equivalently in both the wild-type R603 and mutant R603W backgrounds. Furthermore, substitution with Glu at positions K598 through S601 did not substantially enhance DHA inhibition (Fig. 4 D).

To compare the effect of Arg substitutions on DHA inhibition and polyamine block, we recorded kainate-evoked current during voltage ramps (Fig. 5 A). Polyamine affinity was estimated from normalized conductance versus voltage plots (Fig. 5 B) that were fit with an equation describing inhibition by a permeant blocker (see Materials and methods). Arg substitution at some locations in M3, such as L600 and S619, did not significantly

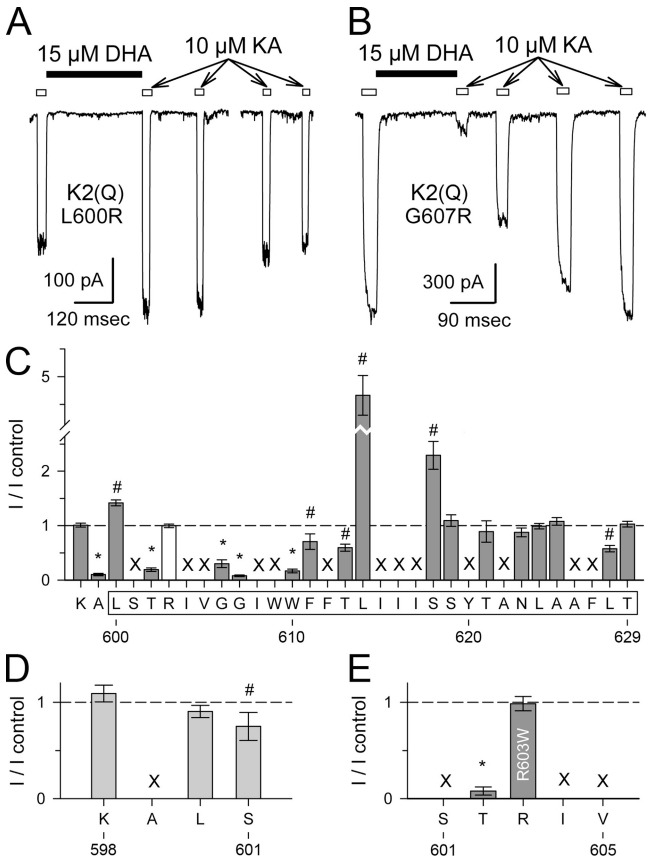

Figure 4. Inhibition and potentiation of GluK2(Q) with Arg substitutions in M3. Whole-cell currents evoked by 10 μM kainate before and after exposure to 15 μM DHA in Con A–treated HEK cells expressing homomeric GluK2(Q) receptors with Arg substitutions at L600 (A) or G607 (B). (C) Current evoked by the first kainate application after exposure to DHA plotted as a fraction of control current before DHA. *, significantly different from Q590 but not Q590R, one-way ANOVA on ranks, $P < 0.05$ by Dunn's method of post-hoc comparison to control. #, significantly different from both Q590 and Q590R, rank sum test, $P < 0.05$. Results for Glu substitution mutants of GluK2(Q) (D) and for Arg substitutions to GluK2(Q) R603W (E). X denotes positions where amino acid substitution resulted in kainate-evoked currents that were too small to analyze.

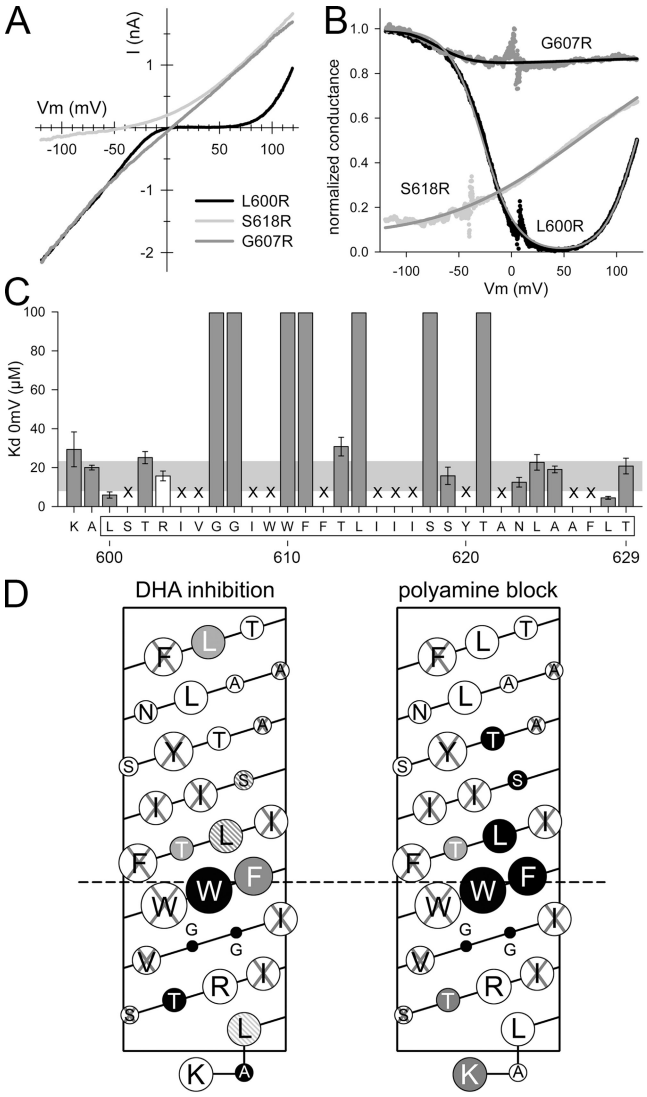

Figure 5. Arg substitutions in M3 disrupt polyamine block. (A) Whole-cell currents evoked by 10 μM kainate during a voltage ramp from −120 to +120 mV for Arg substitutions at L600, G607, and S618 of GluK2(Q). (B) Plots of conductance versus voltage for the three mutants in A normalized to the L600R and G607R values at −120 mV. Smooth curves for L600R and G607R illustrate fits of an equation describing permeant block (see Materials and methods). (C) K_d 0 mV values for polyamine block of Arg substitution mutants from K598 through T629 calculated from Boltzmann fits as illustrated in B. (D) Net diagrams of the M3 helix and adjacent residues. Circle diameter for each residue proportional to side chain volume. (Left) Filled circles indicate locations where Arg substitution allowed strong (black) or intermediate (gray) inhibition by DHA. Hatched circles indicate potentiation by DHA. (Right) Filled circles indicate strong (black) or intermediate (gray) reduction in polyamine block when substituted by Arg. X denotes positions where amino acid substitution resulted in kainate-evoked currents that were too small to analyze. Horizontal dashed line indicates the approximate level of the Q/R site or the top of the M2 loop relative to M3.

alter the bi-rectification that is characteristic of GluK2(Q) channels (Fig. 5, A and C), whereas substitution of G606, G607, W610, or L614 drastically reduced polyamine block, resulting in nearly linear IV relations similar to wild-type edited GluK2(R) (Fig. 5 C); T602R and T613R substitutions yielded more modest reductions in inward rectification. In addition, outwardly rectifying IV relations that reversed between −30 and −50 mV, with cesium glucuronate as the main internal salt, were observed for Arg substitutions at F611, S618, and T621, three positions aligned along one face of the M3 helix at the level of the central cavity (Fig. 5 D). For these constructs, replacing internal cesium glucuronate with CsCl or exchanging sodium glucuronate for external NaCl both reduced outward rectification and shifted the IV reversal potentials to more positive voltages (Fig. S1), indicating that chloride ions in addition to Na, K, and Cs are permeable through the homomeric channels formed by these substitution mutants, as was previously demonstrated for homomeric GluK2(R) (Burnashev et al., 1996). Similar positive shifts in reversal potential with glucuronate substitution, albeit of smaller amplitude, were noted for L614 substitution (see below), which also aligns with F611, S618, and T621 (Fig. 5 D). In contrast, substituting glucuronate for external chloride either caused no significant change (W610R, L624R) or a negative shift in reversal potential (G606R, G607R) for other GluK2(Q) M3 mutants (see below and Table S1).

The plot in Fig. 5 C displays the polyamine affinity calculated for all of the Arg substitutions in M3 that yielded functional channels. Constructs with nearly linear, or outwardly rectifying, IV relations have low apparent polyamine affinity and were designated as Kd(0) > 100 μM to provide a qualitative index of blocking potency (see also Panchenko et al., 2001). Fig. S2 plots polyamine affinities for the M2 Arg substitution mutants from V571-P597 created in our earlier study (Wilding et al., 2008). As illustrated in Fig. 5 D, all of the M3 substitutions that yielded functional channels are distributed along one face of the helix, which is likely to be oriented toward the channel pore, away from the surrounding lipids (see Discussion). At most of these locations Arg substitution reduced polyamine block. Locations in M3 where Arg substitution allowed for DHA to inhibit GluK2(Q) did not directly correlate with side chain volume, but included residues with side chains that were either small (Gly, Thr) or large (Trp). Similarly, the locations where Arg substitution allowed for potentiation by DHA included the small, polar S618, and the larger, hydrophobic L600 and L614. As previously described, removal of positive charge by Ala (Fig. 2) or Trp (Fig. 3) substitution at R603 did not alter polyamine block (Panchenko et al., 2001) or affect susceptibility to DHA inhibition of GluK2(Q).

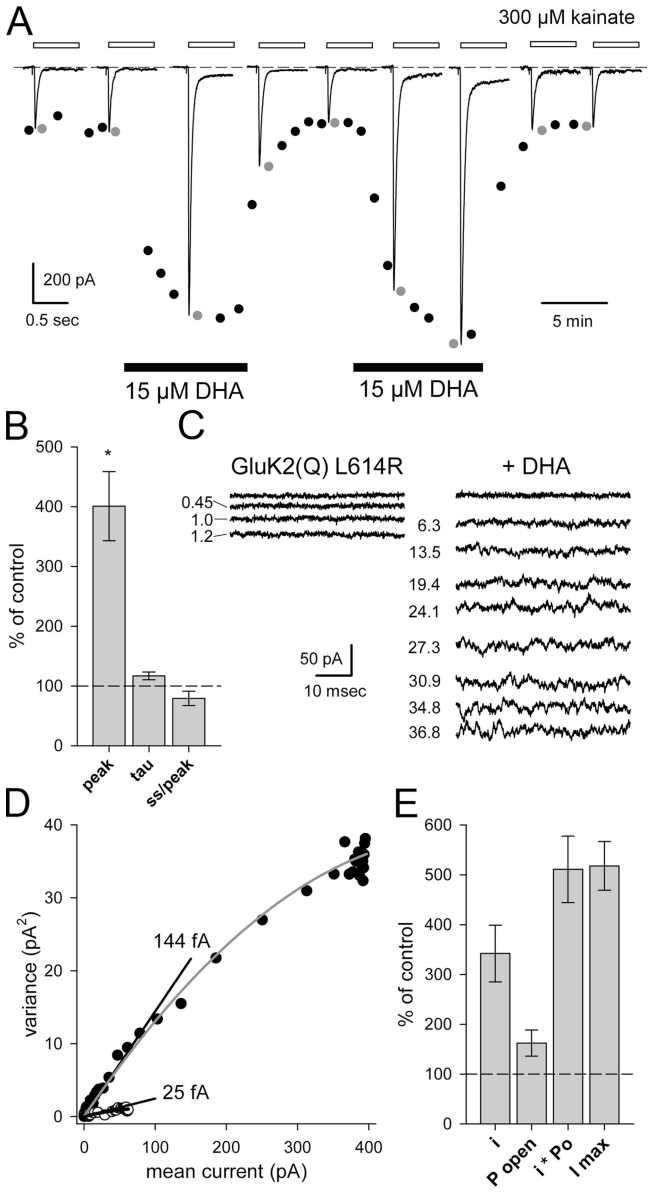

Figure 6. DHA increases unitary current amplitude to potentiate GluK2(Q) L614R. (A) Filled circles plot peak whole-cell current amplitudes evoked by 34 rapid applications of 300 μM kainate to a cell that was not pretreated with ConA. Exposure to 15 μM DHA during the periods indicated by filled bars increased peak inward currents. Gray symbols plot peak whole-cell current amplitude for the nine representative traces that are shown superimposed on the time course plot. (B) Peak current, time constant for a single exponential fit to the decay to steady-state, and steady-state/peak ratio (ss/peak) during exposure to DHA as a percent of control (before and/or after DHA) for experiments as in A, $n = 7$ cells. (C) Whole-cell currents evoked by 10 μM kainate before (left) or during (right) exposure to 15 μM DHA in a Con A–treated cell. (D) Plot of current variance versus mean current for the cell shown in C. Open circles recorded before and filled circles during exposure to DHA. The parabolic smooth curve is the best fit of $\sigma^2 = i*I - I^2/N$, where i is the estimated unitary current amplitude and N is the estimated number of channels. The straight line with slope of 144 fA tangent to the parabolic smooth curve is the estimated i from the parabolic fit for DHA. The line with slope of 25 fA is the estimated i for the control data. (E) Estimated unitary current (i) and open probability (P open) during exposure to kainate and DHA as a percentage of control (kainate alone), $n = 6$ cells. The increase in i and more modest increase in P open together account for the potentiation observed in maximal current.

Potentiation of L614R

To determine how DHA potentiates currents mediated by GluK2(Q) L614R, we used rapid agonist applications to elicit desensitizing currents in transfected HEK cells that were not pretreated with ConA. As illustrated in Fig. 6 A, both peak and steady-state currents were significantly enhanced during periods of exposure to DHA, whereas the exponential time course of current decay (tau) and the ratio of steady-state to peak current were unchanged. These results indicate that potentiation does not require pretreatment with ConA or cause any substantial change in desensitization. Previous work has shown that potentiation of NMDA receptor–mediated currents by AA (Miller et al., 1992) or DHA (Nishikawa et al., 1994) involves an increase in open probability with little or no change in unitary current amplitude. In addition, we found (Wilding et al., 2008) that DHA inhibition of GluK2(R), and of pore-loop Arg substitution mutants of GluK2(Q), entails a decrease in open probability. In contrast, exposure to DHA potentiated GluK2(Q) L614R receptors by significantly increasing unitary current amplitude, combined with a more modest increase in estimated open probability (Fig. 6, C–E). Thus, the potentiation observed for Arg substitution mutants in M3 primarily involves a change in ion conductance through open channels, rather than a change in gating.

Consistent with this idea, we noted a positive shift in reversal potential during exposure to DHA for currents mediated by GluK2(Q) L614R and S618R as well as the Lys substitution L614K (Fig. 7 and Fig. S1). In addition, potentiation by DHA was somewhat weaker for outward currents recorded at positive membrane potentials than for inward currents recorded at negative potentials (Fig. 7 and Fig. S1); for L614R, L614K, and S618K potentiation by DHA at +100mV was 67 ± 9%, 62 ± 9%, and 80 ± 13% of that at −100 mV, respectively, whereas S618R showed even less potentiation at positive potentials (34 ± 8%). With asymmetric chloride concentrations, much of the outward current at positive potentials represents inward flux of chloride. Together, these results suggest that DHA modulation of channels with basic side chains at position 614 or 618 involves a reduction in the chloride permeability relative to control. From the shifts in reversal potential, we estimate 58 ± 5% (L614R, $n = 16$), 13 ± 8% (L614K, $n = 34$), and 27 ± 5% (S618R, $n = 8$) reductions in relative chloride permeability during modulation by DHA; exposure to DHA did not significantly change reversal potential for GluK2(Q) S618K (P = 0.49, $n = 8$).

Arginine substitutions in M1

Although the M1 helix is positioned further from the conducting pore than M3, many channels with Arg substitutions in M1 produced measurable whole-cell currents (Fig. 8). None of the M1 Arg substitutions that we tested resulted in potentiation after DHA exposure. All of the locations where Arg substitution allowed for strong DHA inhibition of GluK2(Q) were on one face of the M1 helix (Fig. 8 C) and included large (Leu), small (Cys, Ser), polar (Cys, Ser), and nonpolar (Val, Leu) residues. Substitution at several of these locations also produced strong (C540, V543) or modest (S544, L547) reductions in polyamine block (K_d 0 mV ~ 20–40 μM); however, Arg substitution at V546, which essentially eliminated polyamine block (K_d 0 mV > 100 μM), had no effect on DHA inhibition (Fig. 8 B).

In the GluA2 crystal structure, the position homologous to V549 is the last residue of the M1 helix, and electron density was not resolved for residues past the position homologous to A551 (Sobolevsky et al., 2009). Thus, the spatial arrangement of residues immediately downstream of A551 remains uncertain. If the M1 helix of GluK2 extends for one to two more turns beyond position 551, then additional locations where Arg substitution supports strong DHA inhibition (A551 and S554) would align along the same face as the four residues further up M1 (see Fig. 8 C). Alternatively, Arg substitution at these specific positions within the cytoplasmic M1 to M2 turret loop may alter pore conformation similar to substitutions within the M1, M2, and M3 helices.

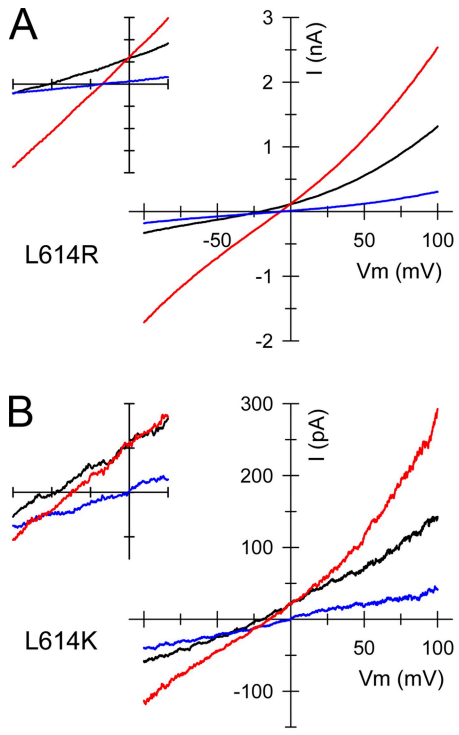

Figure 7. Potentiation of GluK2(Q) L614R and L614K associated with a positive shift in reversal potential. Whole-cell currents elicited by 10 μM kainate between −100 and +100 mV as the membrane potential was ramped at ~1 mV/ms; internal cesium glucuronate. (A) Kainate-evoked current mediated by GluK2(Q) L614R before (black) and after (red) exposure to DHA using external NaCl. Following recovery from DHA potentiation, kainate-evoked current was recorded using extracellular sodium glucuronate (blue). (B) Similar experiment for GluK2(Q) L614K.

DHA modulation without spermine

To test for possible interaction between polyamines and DHA in regulating GluK2 we performed a limited number of experiments in which spermine was not added to the internal solution and intracellular ATP was elevated to 20 mM to buffer endogenous polyamines (Rozov et al., 1998). Similar to control recordings with 20 μM spermine and 5 mM ATP internal, DHA had minimal effect on GluK2(Q), inhibited GluK2(R), and potentiated GluK2(Q) L614R and S618R under nominally polyamine-free conditions, suggesting that cytoplasmic polyamines are not required for channels to be modulated by DHA.

DISCUSSION

Our results identify three surfaces along the M1, M2, and M3 helices where substitution with arginine at any one of 22 locations renders GluK2(Q) channels susceptible to strong (Fig. 9, red) or intermediate (Fig. 9, yellow) inhibition by DHA. Together, these three surfaces delineate the interface where the M2 helix is likely to make close contact with the anti-parallel M1 and M3 helices. Insertion of positive charge at almost any location within this interface, including Q to R substitution by RNA editing of wild-type subunits, changes the contact between M2 and M1/M3, altering the relative motion of these helices when channels open in the presence of DHA. Our results further demonstrate only a partial overlap in the M2 locations where Ala, Trp, or Arg substitutions affect DHA inhibition, and positions where substitution affects polyamine block. Trp substitutions in M2 enhanced DHA inhibition and reduced polyamine block when the large Trp side chain replaced a smaller wild-type residue (G, A, S, T, N), whereas Trp substitution for larger residues (F, L, V) had little or no effect, except near the carboxy-terminal end of M2 immediately preceding the Q/R site. Ala substitution enhanced DHA inhibition at only two locations in M2, T576 and F583, both of which are on the side of the pore helix predicted to face directly toward M1 and M3. Interestingly, T576, located near the opposite end of the pore helix from the Q/R site, is the only position where all three substitutions (A, W, and R) enhanced DHA inhibition and reduced polyamine block.

Our results with Arg substitution in the M3 helix identified three locations where kainate-evoked currents were potentiated by application of DHA (Fig. 9, blue).

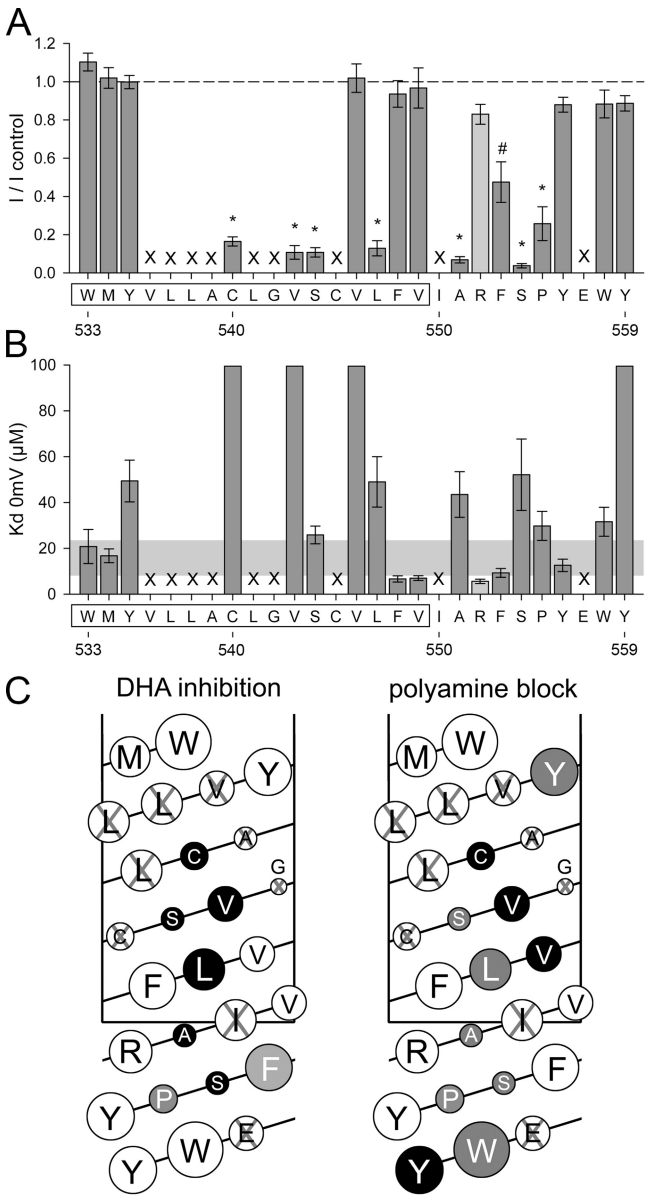

Figure 8. Arg substitution along one face of M1 supports DHA inhibition of GluK2(Q). (A) Current evoked by the first kainate application after exposure to DHA plotted as a fraction of control current before DHA. *, significantly different from Q590 but not Q590R, one-way ANOVA on ranks, $P < 0.05$ by Dunn's method of post-hoc comparison to control. #, significantly different from both Q590 and Q590R, rank sum test, $P < 0.05$. (B) K_d 0 mV values for polyamine block of Arg substitution mutants from W533 through Y559 calculated from Boltzmann fits as illustrated in Fig. 5 B. (C) Net diagrams of the M1 helix. Circle diameter for each residue proportional to side chain volume. (Left) Filled circles indicate locations where Arg substitution allowed strong (black) or intermediate (gray) inhibition by DHA. (Right) Filled circles indicate strong (black) or intermediate (gray) reduction in polyamine block when substituted by Arg. X denotes positions where amino acid substitution resulted in kainate-evoked currents that were too small to analyze.

The weakest potentiation was observed for GluK2(Q) L600R, which is positioned on the cytoplasmic end of M3, below the interface where M2 contacts M3. Significantly stronger potentiation was observed for Arg substitutions at L614 and S618, which are predicted to point into the central cavity just beyond the tip of the pore loop midway between the intracellular and extracellular ends of the M3 helix. Importantly, the potentiation of GluK2(Q) L614R was shown to be largely a result of increased unitary current amplitude, with a more modest increase in estimated open probability. This stands in sharp contrast to DHA potentiation of NMDA receptor channels and DHA inhibition of GluK2(R), which exclusively involve changes in P_{open} (Nishikawa et al., 1994; Wilding et al., 2008). Thus, the mechanism of potentiation for M3 mutant GluK2(Q) homomeric channels appears to be fundamentally different from modulation of wild-type NMDA receptors and GluK2(R).

Subunits with Arg or Lys substituted for L614 or S618, or with Arg substitutions at F611 or T621, displayed increased permeability to Cl ions, as evidenced by positive shifts in reversal potential when CsCl was substituted for internal cesium glucuronate or when sodium glucuronate replaced extracellular NaCl. All of these residues are predicted to face the central cavity, at least when the channels are open (see below). Substitution with positively charged side chains at these locations, as well as G606, G607, and W610, also eliminated block by cytoplasmic polyamines. Previous work by Burnashev et al. (1996) demonstrated significant chloride permeability for homomeric wild-type GluK2(R) channels (P_{Cl}/P_{Cs} = 0.74). In addition, our earlier Arg scan of pore-loop residues (Wilding et al., 2008) showed that between V571 and P597 residues with positively charged side chains supported chloride permeation only when substituted at position 590, the Q/R site, which is believed to point up into the cavity from the apex of the pore loop (Sobolevsky et al., 2009). Collectively, these results are consistent with experiments on other channels of the pore-loop superfamily that have highlighted the importance of residues facing the central cavity (Doyle et al., 1998) in determining channel permeation properties (Yi et al., 2001; Kühn et al., 2007) and susceptibility to block by polyamines (Shyng et al., 1997) or divalent ions (Lu and MacKinnon, 1994). The fact that DHA potentiation of L614R results primarily from an increase in ion conductance and is associated with an apparent change in relative chloride permeability, suggests that DHA changes the relative energy barriers for flux of chloride and cations, possibly by altering the orientation of M3 in the open state and repositioning the substituted side chains away from the pore axis.

An important difference between channel modulation by DHA and block by cytoplasmic polyamines is that polyamines occupy the conductance pathway, causing channel block that is strongly voltage dependent (Bowie and Mayer, 1995; Kamboj et al., 1995; Koh et al., 1995). In contrast, DHA modulation exhibits little or no voltage dependence (Wilding et al., 2005) and likely

involves changes within the membrane, either displacement of annular lipids surrounding each channel (Grossfield et al., 2006; Powl and Lee, 2007) or alterations in bulk membrane properties (Casado and Ascher, 1998; Bruno et al., 2007). Despite this apparent difference in mechanism, our results demonstrate broad overlap in structural requirements for regulation. Of the 66 locations where substitution mutants expressed as functional homomeric channels, nearly half (47%) exhibited both a reduction in polyamine block and an increase in modulation by DHA for at least one of the substituted amino acids (A, R, or W). Fewer locations showed selective regulation by either polyamine block (21%) or DHA modulation (9%) alone, and substitution had no significant effect on block or modulation at roughly a quarter of all locations that allowed functional expression (23%).

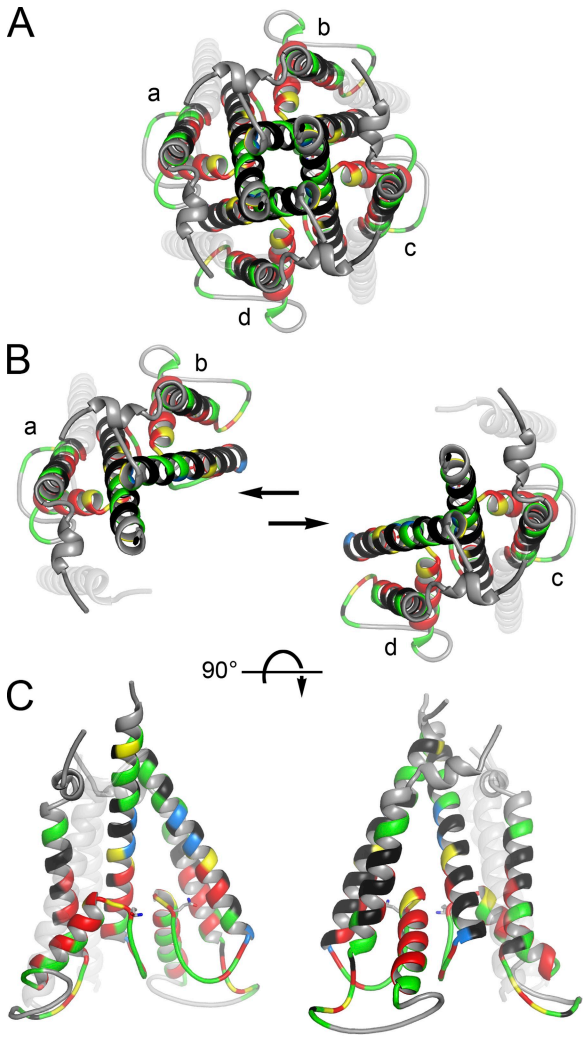

Figure 9. Locations where Arg substitution regulates fatty acid inhibition and potentiation. Homology model of the transmembrane portions of GluK2(Q) based on the x-ray crystal structure of GluA2. (A) View down the central axis of the pore from outside the cell. (B) Same orientation as A, but with the a, b and c, d subunit pairs separated by lateral displacement. (C) Side view of the subunit pairs in B, after 90° rotation, illustrating residues that face the pore (left) or surrounding lipids (right). Locations where Arg substitution promoted strong or intermediate inhibition by DHA are colored red and yellow, respectively. Green indicates positions where Arg substitution did not alter susceptibility of GluK2(Q) to DHA. Little or no whole-cell current was elicited from subunits with Arg substituted a locations colored black. Blue indicates the three Arg substitution positions in M3 where exposure to DHA resulted in potentiation of whole-cell currents. Residues colored gray were not substituted in this study. M4 helices are semi-transparent, for clarity.

In K channels the inner helix bundle crossing and central cavity face the cytoplasm (Doyle et al., 1998). K channel block involves entry of polyamines into the central cavity (Phillips and Nichols, 2003) and is sensitive to placement of charged residues along the inner helix (Kurata et al., 2004). In contrast, the inverted orientation of glutamate receptor channels (Bennett and Dingledine, 1995; Hollmann et al., 1994) means that cytoplasmic polyamines would need to pass through the selectivity filter to access the central cavity, which faces the extracellular solution. For both K channels (Lopatin and Nichols, 1996) and glutamate receptors (Bähring et al., 1997), the potency of polyamine block is reduced by permeant ion flux (but see Rozov et al., 1998). In addition, detailed kinetic analysis by Mayer and colleagues (Bowie et al., 1998) provided evidence for block of both closed and open conformations of GluK2(Q) by cytoplasmic polyamines, although the lack of voltage dependence to closed channel block suggested that polyamines did not penetrate far into the membrane field in the closed state. Previous analysis of the effect of amino acid substitutions on glutamate receptor polyamine block has focused on the pore loop and selectivity filter where polyamines are most likely to be retained (Panchenko et al., 2001), and on adjacent locations on the cytoplasmic face of the channel where substituted residues may repel polyamines from approaching the pore. Our results show that polyamine block is eliminated by substitutions in the central cavity far above the selectivity filter. For example, T621 is located at the distal end of the cavity just before the M3 helix bundle crossing (Sobolevsky et al., 2009), yet T621R substitution drastically reduced polyamine block. Permeability to chloride was a feature of some, but not all, of the M3 substitutions that eliminated polyamine block. Thus, influx of extracellular chloride at positive potentials may help to dispel polyamines from the pore; but, apparently such influx is not required. Indeed, there was no evidence for restoration of polyamine block for Arg or Lys substitutions of L614 or S618 when nearly all of the external chloride was replaced with glucuronate. Together, our results indicate that the presence of positively charged side chains along one face of the M3 helix is sufficient to eliminate block.

In contrast to amino acid replacements within the pore loop, subunits with Arg substitutions at several locations in the M1 and M3 helices failed to express as functional channels or produced whole-cell currents that were too small for accurate determination of inhibition after exposure to DHA (Fig. 9, black). Nearly all of the locations where Arg substitution abrogated channel function are predicted to lie along the sides of M1 and M3 that face outward, away from the channel pore, toward the M4 helix or surrounding lipids. However, at several outward-facing locations near the cytoplasmic or extracellular ends of M1 and M3, Arg substitutions were tolerated and did not enhance GluK2(Q) susceptibility to inhibition (Fig. 9, green). In addition, Arg and/or Trp substitutions at several locations along the M2 helix, including L577 and S580, promoted strong DHA inhibition, but in the closed conformation appear to face outward from the pore at the interface between adjacent subunits (Fig. 9 C, right). In AMPA receptors, the subunit junctions have been suggested (Sobolevsky et al., 2009) as potential interaction sites for auxiliary proteins that regulate channel function (Tomita, 2010). Whether accessory proteins specific for kainate receptors, such as the recently identified NETO2 (Zhang et al., 2009), may occupy this position or whether this side of the M2 helix faces directly toward annular lipids remains to be determined.

In the present study, interpretation of our mutagenesis scan is based on homology to the recently published x-ray structure of homomeric GluA2 AMPA receptor channels (Sobolevsky et al., 2009); whereas previous analysis (Panchenko et al., 2001; Kuner et al., 2003; Sobolevsky et al., 2003; Wilding et al., 2008) was referenced to crystal structures of KcsA (Doyle et al., 1998) and other related potassium channels. GluK2 and GluA2 share a much higher proportion of sequence that is either identical or represent conservative substitutions (Keinänen et al., 1990; Egebjerg et al., 1991) than for potassium channel subunits, supporting the use of GluA2 as a superior template. Indeed, the significantly lower primary sequence homology between GluK2 and K channel subunits in the M1 segment, as compared with the region that includes M2 and M3, led us to use a different M1 alignment, offset by six residues, for our previous homology model (Wilding et al., 2008). Independent evidence concerning glutamate receptor M3 helix orientation comes from studies of functional modification of cysteine-substituted channels by methanethiosulfonate reagents (Wollmuth and Sobolevsky, 2004). For the AMPA receptor, GluA1 subunit residues homologous to GluK2 G607, W610, F611, L614, S618, and T621 all were accessible to modification by extracellularly applied methanethiosulfonate reagents when channels were opened by glutamate coapplication (Sobolevsky et al., 2003).

The cytoplasmic loops from M1 to M2 (R552 through V571) and M2 to M3 (Q591 through L595), which includes the selectivity filter downstream of the Q/R site, are not resolved in the x-ray structure of GluA2 (Sobolevsky et al., 2009). Thus, the accuracy of these segments of our model is much less certain, and interpretation of substitutions in these domains must remain tentative until further structural information is available. Also of importance is the fact that GluA2 was crystallized with a competitive antagonist, ZK200775, lodged in the agonist binding site and thus presents the channel in a presumably closed conformation (Sobolevsky et al., 2009). Channel opening is likely to involve movement of M3 and possibly also the M1 helix, which may alter their orientation relative to M2. In particular, opening of K channels (Perozo et al., 1999; Yi et al., 2001) and cyclic nucleotide-gated channels (Flynn and Zagotta, 2001) is thought to involve coordinated rotation of the inner and outer (M3 and M1) helices, which, if it occurs in GluK2 (Sobolevsky et al., 2003, 2004), would reorient residues relative to the central axis of the pore. For example, a backward rotation about the M3 helical axis of approximately ~30° from the closed conformation would position L614 and S618 directly toward the central axis. Given the twofold symmetry of the agonist binding domain dimers (Sobolevsky et al., 2009), equivalent rotation of all four subunits seems unlikely (Sobolevsky et al., 2004), suggesting that only two of the four M3 Arg substitutions in a homomeric tetramer may be essential for altering channel selectivity, polyamine block, and DHA modulation. In addition, differences in ionization state among the four substituted side chains (Root and MacKinnon, 1994) could determine which subunit pair plays the greater role in influencing channel properties.

In summary, we have now identified >30 gain-of-function substitutions that render GluK2(Q) susceptible to modulation by cis-unsaturated fatty acids. Our results do not resolve whether DHA regulates GluK2 by binding to a specific region of the channel or by altering physical properties of the surrounding membrane, which might be better addressed by loss-of-function mutations that eliminate inhibition of GluK2(R). Nevertheless, our results indicate that, depending on the underlying structure of the channel, exposure to DHA changes the motion of M1 and M3 relative to M2 as channels gate, as well as the final orientation of M3 in the open state. Locations where point mutations render channels susceptible to DHA inhibition are spread along the interface between the pore-loop helix, including the Q/R editing site, and adjacent segments of M1 and M3, suggesting that relative motion of these domains is affected by DHA exposure. In addition, DHA modifies the effect of Arg substitutions located further up the M3 helix at the level of the central cavity, increasing unitary conductance and reducing relative chloride

permeability, which strongly suggests a DHA-induced difference in orientation of M3 to reposition these side chains away from the central axis of the pore in the open state.

We are grateful to Mark Mayer, Steve Heinemann, and Peter Seeburg for providing channel subunit cDNAs and to Colin Nichols and Nazzareno D'Avanzo for critical reading of the manuscript.

This work was supported by the National Institutes of Health (NS30888).

Lawrence G. Palmer served as editor.

Submitted: 29 March 2010
Accepted: 02 July 2010

REFERENCES

Bähring, R., D. Bowie, M. Benveniste, and M.L. Mayer. 1997. Permeation and block of rat GluR6 glutamate receptor channels by internal and external polyamines. *J. Physiol.* 502:575–589. doi:10.1111/j.1469-7793.1997.575bj.x

Beck, C., L.P. Wollmuth, P.H. Seeburg, B. Sakmann, and T. Kuner. 1999. NMDAR channel segments forming the extracellular vestibule inferred from the accessibility of substituted cysteines. *Neuron.* 22:559–570. doi:10.1016/S0896-6273(00)80710-2

Bennett, J.A., and R. Dingledine. 1995. Topology profile for a glutamate receptor: three transmembrane domains and a channel-lining reentrant membrane loop. *Neuron.* 14:373–384. doi:10.1016/0896-6273(95)90293-7

Boland, L.M., and M.M. Drzewiecki. 2008. Polyunsaturated fatty acid modulation of voltage-gated ion channels. *Cell Biochem. Biophys.* 52:59–84. doi:10.1007/s12013-008-9027-2

Bowie, D., and M.L. Mayer. 1995. Inward rectification of both AMPA and kainate subtype glutamate receptors generated by polyamine-mediated ion channel block. *Neuron.* 15:453–462. doi:10.1016/0896-6273(95)90049-7

Bowie, D., G.D. Lange, and M.L. Mayer. 1998. Activity-dependent modulation of glutamate receptors by polyamines. *J. Neurosci.* 18:8175–8185.

Bruno, M.J., R.E. Koeppe II, and O.S. Andersen. 2007. Docosahexaenoic acid alters bilayer elastic properties. *Proc. Natl. Acad. Sci. USA.* 104:9638–9643. doi:10.1073/pnas.0701015104

Burnashev, N., A. Villarroel, and B. Sakmann. 1996. Dimensions and ion selectivity of recombinant AMPA and kainate receptor channels and their dependence on Q/R site residues. *J. Physiol.* 496:165–173.

Casado, M., and P. Ascher. 1998. Opposite modulation of NMDA receptors by lysophospholipids and arachidonic acid: common features with mechanosensitivity. *J. Physiol.* 513:317–330. doi:10.1111/j.1469-7793.1998.317bb.x

Chang, H.R., and C.C. Kuo. 2008. The activation gate and gating mechanism of the NMDA receptor. *J. Neurosci.* 28:1546–1556. doi:10.1523/JNEUROSCI.3485-07.2008

Collingridge, G.L., R.W. Olsen, and M. Spedding. 2009. A nomenclature for ligand-gated ion channels. *Neuropharmacol.* 56:2–5. doi:10.1016/j.neuropharm.2008.06.063

Dingledine, R., K. Borges, D. Bowie, and S.F. Traynelis. 1999. The glutamate receptor ion channels. *Pharmacol. Rev.* 51:7–61.

Doyle, D.A., J. Morais Cabral, R.A. Pfuetzner, A. Kuo, J.M. Gulbis, S.L. Cohen, B.T. Chait, and R. MacKinnon. 1998. The structure of the potassium channel: molecular basis of K+ conduction and selectivity. *Science.* 280:69–77. doi:10.1126/science.280.5360.69

Egebjerg, J., B. Bettler, I. Hermans-Borgmeyer, and S. Heinemann. 1991. Cloning of a cDNA for a glutamate receptor subunit activated by kainate but not AMPA. *Nature.* 351:745–748. doi:10.1038/351745a0

Eswar, N., D. Eramian, B. Webb, M.Y. Shen, and A. Sali. 2008. Protein structure modeling with MODELLER. *Methods Mol. Biol.* 426:145–159. doi:10.1007/978-1-60327-058-8_8

Flynn, G.E., and W.N. Zagotta. 2001. Conformational changes in S6 coupled to the opening of cyclic nucleotide-gated channels. *Neuron.* 30:689–698. doi:10.1016/S0896-6273(01)00324-5

Gawrisch, K., and O. Soubias. 2008. Structure and dynamics of polyunsaturated hydrocarbon chains in lipid bilayers-significance for GPCR function. *Chem. Phys. Lipids.* 153:64–75. doi:10.1016/j.chemphyslip.2008.02.016

Grossfield, A., S.E. Feller, and M.C. Pitman. 2006. A role for direct interactions in the modulation of rhodopsin by omega-3 polyunsaturated lipids. *Proc. Natl. Acad. Sci. USA.* 103:4888–4893. doi:10.1073/pnas.0508352103

Hille, B. 2001. Ion Channels of Excitable Membranes. Third edition. Sinauer Associates, Inc., Sunderland. MA. 814 pp.

Hollmann, M., C. Maron, and S. Heinemann. 1994. N-glycosylation site tagging suggests a three transmembrane domain topology for the glutamate receptor GluR1. *Neuron.* 13:1331–1343. doi:10.1016/0896-6273(94)90419-7

Huettner, J.E. 1990. Glutamate receptor channels in rat DRG neurons: activation by kainate and quisqualate blockade of desensitization by Con A. *Neuron.* 5:255–266. doi:10.1016/0896-6273(90)90163-A

Kamboj, S.K., G.T. Swanson, and S.G. Cull-Candy. 1995. Intracellular spermine confers rectification on rat calcium-permeable AMPA and kainate receptors. *J. Physiol.* 486:297–303.

Keinänen, K., W. Wisden, B. Sommer, P. Werner, A. Herb, T.A. Verdoorn, B. Sakmann, and P.H. Seeburg. 1990. A family of AMPA-selective glutamate receptors. *Science.* 249:556–560. doi:10.1126/science.2166337

Koh, D.S., N. Burnashev, and P. Jonas. 1995. Block of native Ca(2+)-permeable AMPA receptors in rat brain by intracellular polyamines generates double rectification. *J. Physiol.* 486:305–312.

Kovalchuk, Y., B. Miller, M. Sarantis, and D. Attwell. 1994. Arachidonic acid depresses non-NMDA receptor currents. *Brain Res.* 643:287–295. doi:10.1016/0006-8993(94)90035-3

Kühn, F.J.P., G. Knop, and A. Lückhoff. 2007. The transmembrane segment S6 determines cation versus anion selectivity of TRPM2 and TRPM8. *J. Biol. Chem.* 282:27598–27609. doi:10.1074/jbc.M702247200

Kuner, T., L.P. Wollmuth, A. Karlin, P.H. Seeburg, and B. Sakmann. 1996. Structure of the NMDA receptor channel M2 segment inferred from the accessibility of substituted cysteines. *Neuron.* 17:343–352. doi:10.1016/S0896-6273(00)80165-8

Kuner, T., C. Beck, B. Sakmann, and P.H. Seeburg. 2001. Channel-lining residues of the AMPA receptor M2 segment: structural environment of the Q/R site and identification of the selectivity filter. *J. Neurosci.* 21:4162–4172.

Kuner, T., P.H. Seeburg, and H.R. Guy. 2003. A common architecture for K+ channels and ionotropic glutamate receptors? *Trends Neurosci.* 26:27–32. doi:10.1016/S0166-2236(02)00010-3

Kurata, H.T., L.R. Phillips, T. Rose, G. Loussouarn, S. Herlitze, H. Fritzenschaft, D. Enkvetchakul, C.G. Nichols, and T. Baukrowitz. 2004. Molecular basis of inward rectification: polyamine interaction sites located by combined channel and ligand mutagenesis. *J. Gen. Physiol.* 124:541–554. doi:10.1085/jgp.200409159

Lopatin, A.N., and C.G. Nichols. 1996. [K+] dependence of polyamine-induced rectification in inward rectifier potassium channels (IRK1, Kir2.1). *J. Gen. Physiol.* 108:105–113. doi:10.1085/jgp.108.2.105

Lu, Z., and R. MacKinnon. 1994. Electrostatic tuning of Mg^{2+} affinity in an inward-rectifier K^+ channel. *Nature.* 371:243–246. doi:10.1038/371243a0

Lundbaek, J.A. 2008. Lipid bilayer-mediated regulation of ion channel function by amphiphilic drugs. *J. Gen. Physiol.* 131:421–429. doi:10.1085/jgp.200709948

Margeta-Mitrovic, M., Y.N. Jan, and L.Y. Jan. 2000. A trafficking checkpoint controls GABA(B) receptor heterodimerization. *Neuron.* 27:97–106. doi:10.1016/S0896-6273(00)00012-X

Meves, H. 2008. Arachidonic acid and ion channels: an update. *Br. J. Pharmacol.* 155:4–16. doi:10.1038/bjp.2008.216

Miller, B., M. Sarantis, S.F. Traynelis, and D. Attwell. 1992. Potentiation of NMDA receptor currents by arachidonic acid. *Nature.* 355: 722–725. doi:10.1038/355722a0

Nishikawa, M., S. Kimura, and N. Akaike. 1994. Facilitatory effect of docosahexaenoic acid on N-methyl-D-aspartate response in pyramidal neurones of rat cerebral cortex. *J. Physiol.* 475:83–93.

Panchenko, V.A., C.R. Glasser, and M.L. Mayer. 2001. Structural similarities between glutamate receptor channels and K(+) channels examined by scanning mutagenesis. *J. Gen. Physiol.* 117:345–360. doi:10.1085/jgp.117.4.345

Perozo, E., D.M. Cortes, and L.G. Cuello. 1999. Structural rearrangements underlying K^+-channel activation gating. *Science.* 285:73–78. doi:10.1126/science.285.5424.73

Phillips, L.R., and C.G. Nichols. 2003. Ligand-induced closure of inward rectifier Kir6.2 channels traps spermine in the pore. *J. Gen. Physiol.* 122:795–804. doi:10.1085/jgp.200308953

Phillips, R., T. Ursell, P. Wiggins, and P. Sens. 2009. Emerging roles for lipids in shaping membrane-protein function. *Nature.* 459:379–385. doi:10.1038/nature08147

Powl, A.M., and A.G. Lee. 2007. Lipid effects on mechanosensitive channels. *Current Topics in Membranes.* 58:151–178. doi:10.1016/S1063-5823(06)58006-8

Roberts-Crowley, M.L., T. Mitra-Ganguli, L. Liu, and A.R. Rittenhouse. 2009. Regulation of voltage-gated Ca2+ channels by lipids. *Cell Calcium.* 45:589–601. doi:10.1016/j.ceca.2009.03.015

Root, M.J., and R. MacKinnon. 1994. Two identical noninteracting sites in an ion channel revealed by proton transfer. *Science.* 265:1852–1856. doi:10.1126/science.7522344

Rozov, A., Y. Zilberter, L.P. Wollmuth, and N. Burnashev. 1998. Facilitation of currents through rat Ca^{2+}-permeable AMPA receptor channels by activity-dependent relief from polyamine block. *J. Physiol.* 511:361–377. doi:10.1111/j.1469-7793.1998.361bh.x

Sali, A., and T.L. Blundell. 1993. Comparative protein modeling by satisfaction of spatial restraints. *J. Mol. Biol.* 234:779–815. doi:10.1006/jmbi.1993.1626

Shen, M.Y., and A. Sali. 2006. Statistical potential for assessment and prediction of protein structures. *Protein Sci.* 15:2507–2524. doi:10.1110/ps.062416606

Shyng, S., T. Ferrigni, and C.G. Nichols. 1997. Control of rectification and gating of cloned KATP channels by the Kir6.2 subunit. *J. Gen. Physiol.* 110:141–153. doi:10.1085/jgp.110.2.141

Sobolevsky, A.I., L. Rooney, and L.P. Wollmuth. 2002. Staggering of subunits in NMDAR channels. *Biophys. J.* 83:3304–3314. doi:10.1016/S0006-3495(02)75331-9

Sobolevsky, A.I., M.V. Yelshansky, and L.P. Wollmuth. 2003. Different gating mechanisms in glutamate receptor and K+ channels. *J. Neurosci.* 23:7559–7568.

Sobolevsky, A.I., M.V. Yelshansky, and L.P. Wollmuth. 2004. The outer pore of the glutamate receptor channel has 2-fold rotational symmetry. *Neuron.* 41:367–378. doi:10.1016/S0896-6273(04)00008-X

Sobolevsky, A.I., M.P. Rosconi, and E. Gouaux. 2009. X-ray structure, symmetry and mechanism of an AMPA-subtype glutamate receptor. *Nature.* 462:745–756. doi:10.1038/nature08624

Sigworth, F.J. 1980. The variance of sodium current fluctuations at the node of Ranvier. *J. Physiol.* 307:97–129.

Tomita, S. 2010. Regulation of ionotropic glutamate receptors by their auxiliary subunits. *Physiology (Bethesda).* 25:41–49.

Wilding, T.J., M.D. Womack, and E.W. McCleskey. 1995. Fast, local signal transduction between μ opioid receptor and Ca^{2+} channels. *J. Neurosci.* 15:4124–4132.

Wilding, T.J., Y.H. Chai, and J.E. Huettner. 1998. Inhibition of rat neuronal kainate receptors by cis-unsaturated fatty acids. *J. Physiol.* 513:331–339. doi:10.1111/j.1469-7793.1998.331bb.x

Wilding, T.J., Y. Zhou, and J.E. Huettner. 2005. Q/R site editing controls kainate receptor inhibition by membrane fatty acids. *J. Neurosci.* 25:9470–9478. doi:10.1523/JNEUROSCI.2826-05.2005

Wilding, T.J., E. Fulling, Y. Zhou, and J.E. Huettner. 2008. Amino acid substitutions in the pore helix of GluR6 control inhibition by membrane fatty acids. *J. Gen. Physiol.* 132:85–99. doi:10.1085/jgp.200810009

Wo, Z.G., and R.E. Oswald. 1995. Unraveling the modular design of glutamate-gated ion channels. *Trends Neurosci.* 18:161–168. doi:10.1016/0166-2236(95)93895-5

Wollmuth, L.P., and A.I. Sobolevsky. 2004. Structure and gating of the glutamate receptor ion channel. *Trends Neurosci.* 27:321–328. doi:10.1016/j.tins.2004.04.005

Wood, M.W., H.M. VanDongen, and A.M. VanDongen. 1995. Structural conservation of ion conduction pathways in K channels and glutamate receptors. *Proc. Natl. Acad. Sci. USA.* 92:4882–4886. doi:10.1073/pnas.92.11.4882

Yi, B.A., Y.F. Lin, Y.N. Jan, and L.Y. Jan. 2001. Yeast screen for constitutively active mutant G protein-activated potassium channels. *Neuron.* 29:657–667. doi:10.1016/S0896-6273(01)00241-0

Zhang, W., F. St-Gelais, C.P. Grabner, J.C. Trinidad, A. Sumioka, M. Morimoto-Tomita, K.S. Kim, C. Straub, A.L. Burlingame, J.R. Howe, and S. Tomita. 2009. A transmembrane accessory subunit that modulates kainate-type glutamate receptors. *Neuron.* 61:385–396. doi:10.1016/j.neuron.2008.12.014